Nuclear Physics B152 (1979) 365–375

CHARGED CURRENT ELASTIC ANTINEUTRINO INTERACTIONS IN PROPANE

N. ARMENISE, O. ERRIQUEZ, M.T. FOGLI MUCIACCIA, S. NUZZO and F. RUGGIERI
Istituto di Fisica dell'Università and INFN, Bari, Italy

A. HALSTEINSLID, K. MYKLEBOST, A. ROGNEBAKKE and O. SKJEGGESTAD
Institute of Physics, University of Bergen, Norway

S. BONETTI, D. CAVALLI, M.C. PERNIGONI, A. PULLIA and M. ROLLIER
Istituto di Fisica dell'Università and INFN, Milano, Italy

J.P. ENGEL, B. ESCOUBES, J.L. GUYONNET, D. HUSS *, J.L. RIESTER and M. SCHAEFFER
Centre de Recherches Nucleaires et Université Louis Pasteur, Strasbourg, France

D. ALLASIA, V. BISI, D. GAMBA, A. MARZARI CHIESA, L. RICCATI and A. ROMERO
Istituto di Fisica dell'Università and INFN, Torino, Italy

F.W. BULLOCK, R.C.W. HENDERSON **, T.W. JONES and F. RAMZAN
University College London, London, UK

Received 30 November 1978
(Revised 15 February 1979)

A sample of 766 antineutrino charged current elastic events has been used to extract the variation of the elastic cross section with antineutrino energy and the distribution of dN/dq^2. The best fit value for the parameter M_A obtained from these measurements is $M_A = 0.91 \pm 0.04$ GeV/c^2 for $M_V = 0.84$ GeV/c^2. A simultaneous determination of M_A and M_V gives $M_A = 0.94 \pm 0.07$, $M_V = 0.81 \pm 0.03$.

* Also at Université de Haute-Alsace, Mulhouse, France
** Supported by SRC Studentship.

1. Introduction

We present here the results of an analysis on 766 examples of the quasi-elastic antineutrino charged current interaction

$$\bar{\nu}_\mu + p \to \mu^+ + n \qquad (1)$$

in a light propane/freon mixture. Previous work on this topic has been performed in heavy freon only [1]. The parameter M_A in the dipole representation of the axial form factor has been determined by two essentially independent methods, *viz.*, from the variation of the elastic cross section, σ, with antineutrino energy and from the distribution dN/dq^2, q^2 being the 4-momentum transfer.

2. Experimental procedure

2.1. Beam, chamber, runs

The heavy liquid bubble chamber Gargamelle was exposed to the CERN-PS antineutrino beam for a total amount of $1.57 \cdot 10^{18}$ protons on the target. The antineutrino spectrum is shown in fig. 1.

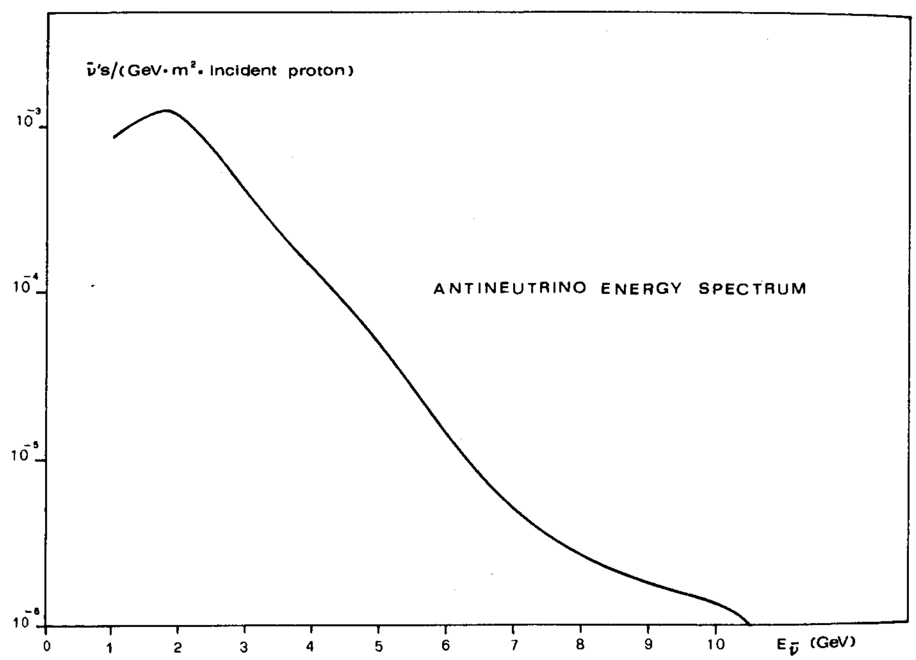

Fig. 1. Antineutrino energy spectrum.

Table 1
Relevant data related to the experimental conditions of the present experiment

Runs	I + II	III + IV	Total or average
Total number of accelerated protons on target	$0.55 \cdot 10^{18}$	$1.02 \cdot 10^{18}$	$1.57 \cdot 10^{18}$
Pictures scanned	$125 \cdot 10^3$	$180 \cdot 10^3$	$305 \cdot 10^3$
Molar proportion C_3H_8/CF_3Br	91/9	85/15	87/13
Density (g/cm^3)	0.515	0.617	0.581
Radiation length (cm)	64	47	53
Free protons/cm^3	$4.29 \cdot 10^{22}$	$4.34 \cdot 10^{22}$	$4.32 \cdot 10^{22}$
Bound protons/cm^3	$12.92 \cdot 10^{22}$	$15.86 \cdot 10^{22}$	$14.83 \cdot 10^{22}$
Bound neutrons/cm^3	$13.54 \cdot 10^{22}$	$16.90 \cdot 10^{22}$	$15.73 \cdot 10^{22}$
$\bar{\nu}$'s in the fiducial volume of Gargamelle	$1.0 \cdot 10^{15}$	$1.9 \cdot 10^{15}$	$2.9 \cdot 10^{15}$

Four runs were carried out, between summer 1974 and 1975. The chamber was filled with a mixture of C_3H_8–CF_3Br. The proportion of the two liquids in the different runs, together with all relevant parameters are given in table 1.

A total of $3 \cdot 10^5$ pictures were scanned for any type of interaction and ≈70% of the film was scanned twice. The scanning efficiency for elastic events was found to be 83% after a single scan and 97% after a second scan.

2.2. Selection of the events

When reaction (1) takes place on a free proton, one expects the event to appear as an isolated μ^+ track originating in the liquid. However, in our mixture, ≈77% of the elastic events take place on bound protons. Then, the emerging neutron can interact in nuclear matter producing other charged secondaries, i.e.,

$$\bar{\nu} + (A, Z) \rightarrow \mu^+ + \text{hadronic secondaries} + (A', Z') , \qquad (2)$$

where (A, Z) indicates a nucleus of A nucleons and electric charge Z. Hadronic secondaries can be: (a) slow nuclear splinters of evaporation protons (kinetic energy < 30 MeV) following nuclear de-excitation; (b) energetic protons or pions resulting from a direct neutron-nucleon collision in the parent nucleus.

In order to minimize the loss of genuine events and the inclusion of backgrounds in our sample, the events were selected according to the topological and kinematical requirements described below.

(I) Topological requirements were that for each event:

(a) the vertex of the primary $\bar{\nu}$ interaction should be inside a fiducial volume of ≈3 m^3 compared to a visible volume of ≈8 m^3;

(b) there should be only one μ^+ candidate, i.e., a positive non-interacting particle leaving the chamber, or decaying at rest inside the chamber;

(c) there should be no other track, except stopping positive tracks with a maximum range corresponding to a proton of kinetic energy = 30 MeV;

(d) there should be no visible γ nor V^0 pointing to the primary vertex in the visible volume.

(II) Kinematical requirements were:

(a) the calculated $\bar{\nu}$ energy $E_{\bar{\nu}} \geqslant 1$ GeV. Only ≈10% of the events had a correlated neutron star in the same frame giving a successful 2C fit. The antineutrino energy was therefore computed from the muon track and the known antineutrino direction. The target proton of reaction (1) was assumed to be at rest, and the kinematic parameters of the unseen neutron were calculated by balancing energy and momentum. The mean error on $E_{\bar{\nu}}$ due to ignoring the Fermi motion was found to be negligible. It was also verified that this error on $E_{\bar{\nu}}$ does not appreciably modify the q^2 distribution, q^2 being the square of the four-momentum transferred to the nucleon ($q^2 = 2E_{\bar{\nu}}(E_\mu - P_\mu \cos\theta_\mu) - m_\mu^2$);

(b) the muon longitudinal momentum (the component parallel to the $\bar{\nu}$ direction) $P_{\mu_x} \geqslant 0.6$ GeV/c;

(c) the relative error on the muon momentum $\Delta P_\mu / P_\mu \leqslant 20\%$.

The above cuts were applied in order to eliminate or minimize the effects of the following sources of error:

(i) poor knowledge of the $\bar{\nu}$ energy spectrum below 1 GeV;

(ii) neutron background arising from $\bar{\nu}$ interactions in the last part of the shielding;

(iii) entering negative particles interacting in the chamber and for which the direction of motion could not be established;

(iv) neutral current events producing a non-interacting π^+ or proton.

The 776 events selected in this way showed a uniform distribution in the chamber along the antineutrino beam direction indicating that background (ii) had been strongly reduced.

3. Estimate of contamination and losses

The requirements imposed by our selection, whilst excluding a number of genuine events, did not eliminate completely contamination by unwanted events. The extent of both effects was estimated as follows.

(a) Neutral current events with a single positive hadron can simulate a charged current elastic event if the hadron leaves the chamber without interaction. This contamination has been estimated from the observed single π^+ or single proton NC events, i.e., events surviving the kinematical tests listed in sect. 2 and in which the π^+ or proton were seen to interact in the chamber: 28 such events were observed in the same sample of the film. Using the experimental interaction length for pions

Ka Kironh

and protons and the potential length of each track, a contamination of 12 ± 3 events was estimated to be present in our sample.

(b) The reactions $\bar{\nu}p \rightarrow \mu^+ n\pi^0$, $\bar{\nu}n \rightarrow \mu^+ n\pi^-$ and $\bar{\nu}p \rightarrow \mu^+ p\pi^-$ (with the proton of kinetic energy less than 30 MeV) can simulate an elastic charged current interaction if the pion is re-absorbed in the parent nucleus without visible effects other than low-energy protons. This background has been calculated using, for each pion energy, the experimental probability for re-absorption of pions in our propane-freon mixture [2,3] (mean value (17 ± 3)%) and the probability for the interacting pion to produce no fast visible track((30 ± 3)% for π^0's and (54 ± 6)% for π^-'s). The latter figure was directly determined from an analysis of interacting π^-'s, ejected

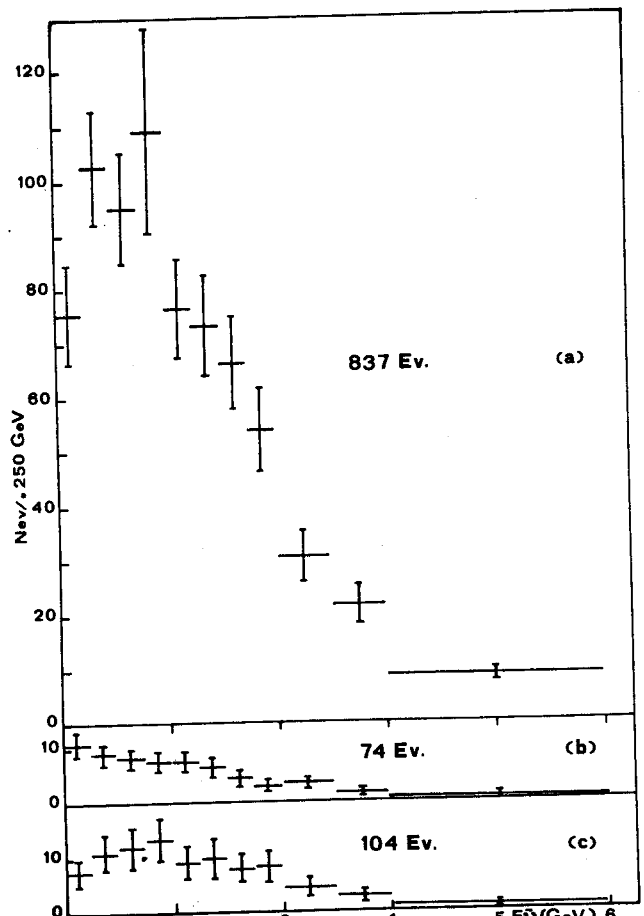

Fig. 2. Energy distribution: (a) selected events corrected for scanning efficiency, (b) background, (c) losses.

from $\bar{\nu}$ interactions observed in this experiment. It is the fraction of them that interact producing only slow protons of kinetic energy <30 MeV. The corresponding value for the π^0 was deduced by assuming charge independence in pion-nucleon interactions [3]. The resulting contamination is 13 ± 3 charged current one π^- events and 11 ± 2 charged current one π^0 events. The background due to 2π charged current events was found negligible by the same procedure.

(c) Single π^0 charged current events can simulate an elastic event also when the π^0 is undetected. This contamination was determined from the number of observed γ's in $\mu^+ + n\gamma$ events. It was concluded that 26 ± 4 events of this type have been included in our sample.

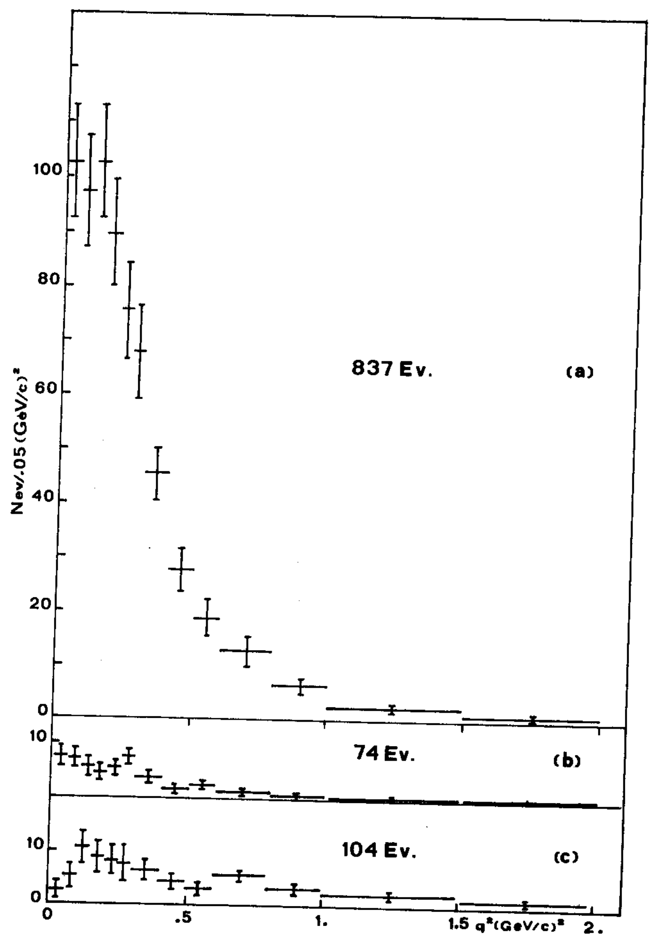

Fig. 3. q^2 distribution: (a) selected events corrected for scanning efficiency, (b) background, (c) losses.

(d) The events $\bar{\nu}p \to \mu^+\Lambda^0$ simulate charged current elastic events when the Λ^0 is unseen because it decays *via* neutral particles or outside the visible volume. From the observed number of events with a Λ^0 a background of 12 ± 3 events was calculated. The background due to undetected K^0's was found to be negligible.

(e) If the produced neutron interacts in the parent nucleus producing a fast visible particle (a proton of kinetic energy >30 MeV or a pion) the event would be excluded from our sample. The probability for such an event to occur has been computed by a Monte Carlo calculation. The cross sections of neutrons on bound nucleons, calculated [4] taking into account the intranuclear cascades generated in the complex nuclei were used. For a given q^2 and a given nucleus the probability of producing an event which would not satisfy the kinematical and topological requirements listed in sect. 2, was computed. It was found that the total number of events to be added to our sample is 104 ± 11.

In figs. 2 and 3 the energy and q^2 distributions of the selected events, corrected only for the scanning efficiency which was tested to be independent of $E_{\bar{\nu}}$ and q^2, are reported. For comparison, the same distributions for the calculated background and losses are also given.

4. Comparison of the experimental results with theory

4.1. Calculation of cross section

In the framework of the classical (V − A) theory, assuming charge symmetry and time reversal invariance, the differential cross section $d\sigma/dq^2$ of reaction (1) is described by the equation *

$$\frac{d\sigma}{dq^2} = \frac{G^2 \cos^2 \vartheta_C M^2}{8\pi E_{\bar{\nu}}^2}\left\{A(q^2) - \frac{s-u}{M^2}B(q^2) + \left(\frac{s-u}{M^2}\right)^2 C(q^2)\right\}, \qquad (3)$$

where M is the nucleon mass, G the coupling constant, ϑ_C the Cabibbo angle and:

$$s - u = 4E_{\bar{\nu}}M - q^2 - m_\mu^2,$$

$$A = \frac{q^2 + m_\mu^2}{4M^2}\left\{F_V^2\left(\frac{q^2}{M^2} - 4\right) + F_M^2\frac{q^2}{M^2}\left(1 - \frac{q^2}{4M^2}\right) + 4F_VF_M\frac{q^2}{M^2} + F_A^2\left(4 + \frac{q^2}{M^2}\right) - \frac{m_\mu^2}{M^2}\left|(F_V + F_M)^2 + F_A^2\right|\right\},$$

$$B = q^2(F_V + F_M)F_A/M^2, \qquad C = \tfrac{1}{4}(F_V^2 + q^2F_M^2/4M^2 + F_A^2).$$

The pseudoscalar contribution is neglected. The form factors are parametrized in the

* For a complete discussion and the meaning of notations, see ref. [5].

usual dipole form:

$$F_i = \frac{F_i(0)}{(1 + q^2/M_i^2)^2} \; .$$

According to the isotriplet current hypothesis, F_V and F_M are assumed to be identical with the isovector nucleon form factors ($F_V(0) = 1$, $F_M(0) = 3.71$, $M_V = M_M = 0.84$ GeV/c^2). Assuming $F_A(0) = 1.26$ [9] the only free parameter remains M_A.

As in our experiment the target proton of reaction (1) is almost always bound in a nucleus, it is necessary to modify eq. (3) to take into account the effects of Fermi motion and the Pauli exclusion principle for which a simple Fermi gas model was used; in fact, more sophisticated models (like the shell model) do not give appreciably different results [6,7]. Eq. (3) was also corrected for the effects of broadening due to experimental resolution.

4.2. Determination of M_A

A least square fit consisting in minimizing the function $\eta = \Sigma_i (N_i^{\text{th}} - N_i^{\text{exp}})^2 \sigma_i^{-2}$ was used to extract M_A from the experimental data. The analysis was performed on the following distributions:

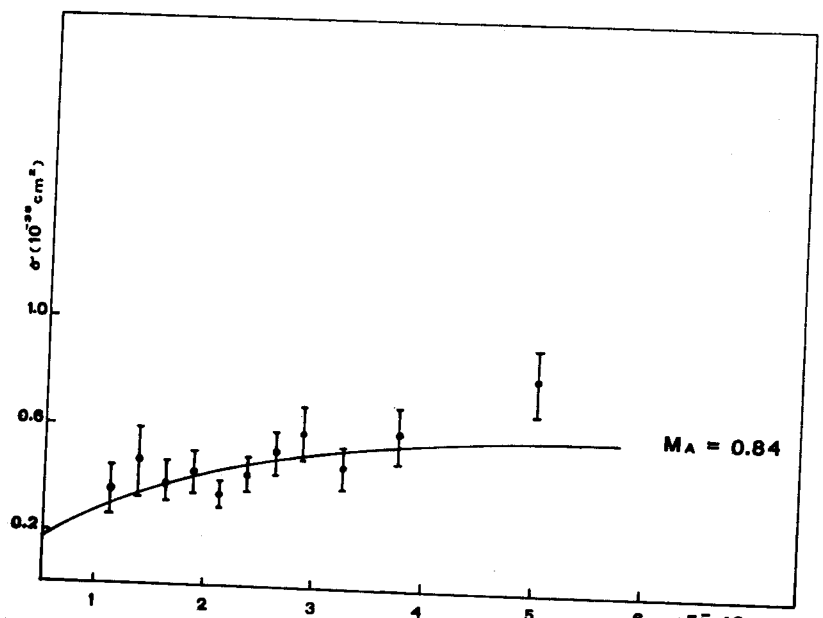

Fig. 4. Total elastic cross section *versus* energy. The curve is the theoretical prediction for our best fitted value of M_A. The error bars indicated here include both statistical and systematic errors.

the total elastic cross section as a function of energy;
the differential distribution dN/dq^2 averaged over the energy spectrum;
the two-dimensional distribution dN/dq^2 *versus* $E_{\bar{\nu}}$.

Figs. 4 and 5 show the total cross section for reaction (1) as a function of energy and the differential distribution dN/dq^2. The curves on the figures are the theoretical curves computed for the best fitted value of M_A (respectively $M_A = 0.84$ GeV/c^2 and $M_A = 0.94$ GeV/c^2) and corrected as said before. The experimental errors include statistical fluctuations, uncertainty on the flux of the $\bar{\nu}$ beam and the corrections mentioned in sect. 3.

As it is evident from figs. 2 and 3, the losses and contaminations (due to second-

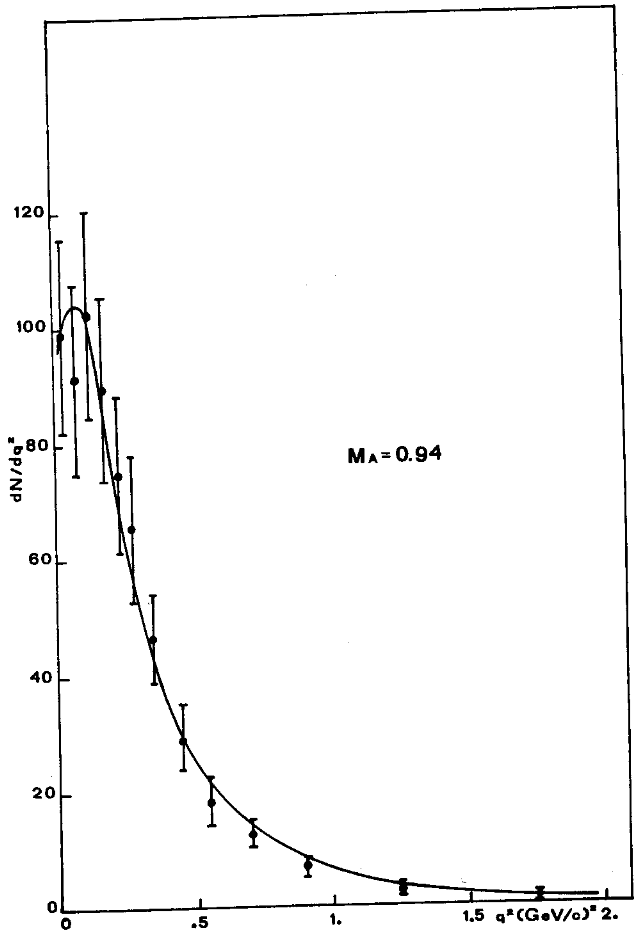

Fig. 5. Differential distribution dN/dq^2 integrated over the energy spectrum between 1 and 10 GeV. The curve is the theoretical prediction for our best fitted value of M_A.

ary nuclear effects which are present when reaction (1) occurs on a bound proton target) are comparably small when $q^2 < 0.6$ (GeV/c)^2. Moreover, the Pauli exclusion principle alters the cross section in a negligible way when $q^2 > 0.15$ (GeV/c)^2.

Thus, the dN/dq^2 distribution inside the interval $0.15 < q^2 < 0.6$ (GeV/c)^2 is relatively error free. The value of M_A obtained from the data within these limits of q^2($M_A = 0.95 \pm 0.07$) is in excellent agreement with those mentioned above.

4.3. *Simultaneous determination of M_A and M_V*

A two-parameter fit, in which both M_A and M_V are allowed to vary, was attempted. The result, obtained from the two-dimensional distribution dN/dq^2 *versus* $E_{\bar{\nu}}$, is shown in fig. 6. The best fit ($\eta = 54$, ND = 47) in the (M_A, M_V) plane is given there, together with the contours corresponding to one and two standard deviations. The value of M_V ($0.81^{+0.02}_{-0.05}$ GeV/c^2) is consistent with the CVC predictions and the value of M_A ($0.94^{+0.08}_{-0.06}$ GeV/c^2) is in agreement with the one-parameter fit of subsect. 4.2.

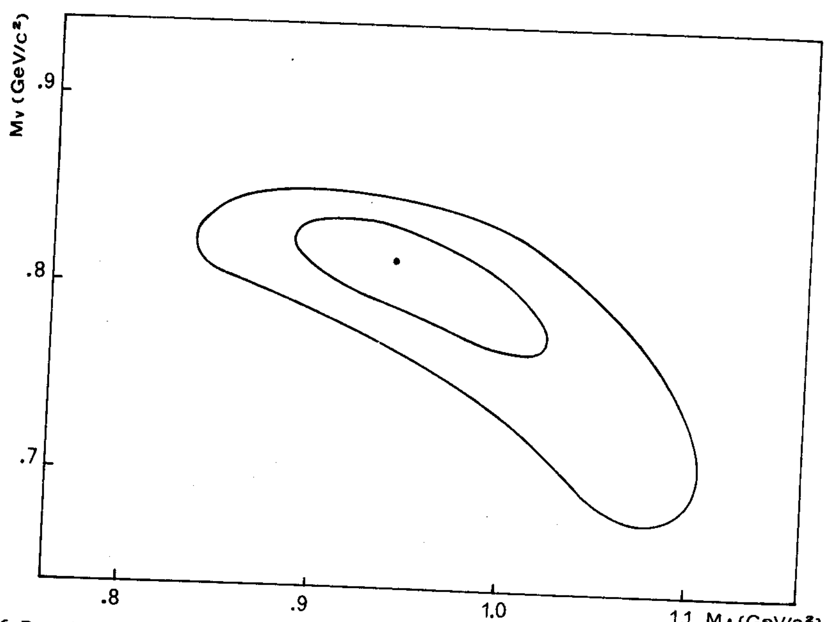

Fig. 6. Best fit in M_A, M_V space. The contours correspond to one and two standard deviations.

Table 2
Results of fits on the parameter M_A

	M_A	η	ND
$\sigma(E_{\bar{\nu}})$	$0.84 \pm ^{0.08}_{0.09}$	9.5	10
dN/dq^2	0.94 ± 0.05	8.5	12
$d\sigma/dq^2(E_{\bar{\nu}})$	0.91 ± 0.04	55	48

5. Conclusions

The analysis of the elastic $\bar{\nu}$ events carried out in this experiment has been used to determine the value of the axial vector form factor parameter M_A both from the total cross section and the q^2 distribution. The results obtained in various ways are listed in table 2.

A combined fit on q^2 *versus* $E_{\bar{\nu}}$ of $d\sigma(q^2, E_{\bar{\nu}})/dq^2$ gives as best fit value:

$$M_A = 0.91 \pm 0.04 \text{ GeV}/c^2$$

for $M_V = 0.84$ GeV/c^2.

A simultaneous determination of M_V and M_A gives

$$M_V = 0.81^{+0.02}_{-0.05}\,, \qquad M_A = 0.94^{+0.08}_{-0.06}\,.$$

Previous determinations of M_A for antineutrinos have been given by Bonetti et al. [1]. They find $M_A = 0.94 \pm 0.17$ GeV/c^2 from the q^2 distribution. Barish et al. [8] find $M_A = 0.95 \pm 0.09$ GeV/c^2, from neutrino quasi-elastic scattering.

References

[1] S. Bonetti et al., Nuovo Cim. 38A (1977) 260.
[2] O. Erriquez et al., Phys. Lett. 73B (1978) 350.
[3] E. Bellotti et al., Nuovo Cim. 14A (1973) 567.
[4] K. Chen et al., Phys. Rev. 166 (1968) 949;
M. Pohl and C. Longuemare, Aachen preprint, to be published.
[5] C.H. Llewellyn Smith, Phys. Reports 3 (1972) 261.
[6] J.S. Bell and C.H. Llewellyn Smith, Nucl. Phys. B28 (1971) 317.
[7] M. Schaeffer and G. Bonneaud, CRN/HE 77-17 (1977).
[8] S.J. Barish et al., Phys. Rev. D16 (1977) 3103.
[9] M.M. Nagels et al., Nucl. Phys. B109 (1976) 1.